Chapter 2
The Geologic Context of Korsi Dora and the Partial Skeleton KSD-VP-1/1

Beverly Z. Saylor, Mulugeta Alene, Alan Deino, Luis Gibert, Yohannes Haile-Selassie, Stephanie M. Melillo, and Gary Scott

Abstract KSD-VP-1/1, a partial skeleton of *Australopithecus afarensis*, was excavated from Pliocene strata at Korsi Dora, 3.3 km southeast of the confluence of the Waki and Mille rivers in the northwestern part of the Woranso-Mille paleoanthropological research site. A tuff collected from ~2.7 m below the fossil horizon, at the bottom of a trench dug 25 m to the east of the fossil excavation, yielded an $^{40}Ar/^{39}Ar$ age of 3.60 ± 0.03 Ma for anorthoclase feldspar. Strata in the trench and the fossil excavation site comprise a single normal magnetozone interpreted as part of the normal subchron C2An.3n, immediately above the Gauss/Gilbert paleomagnetic transition. Geologic mapping and tephrochemical analyses combined with paleomagnetic data place the fossil horizon and the trench section into local and regional stratigraphic context by constraining the partial skeleton to be younger than the Kilaytoli tuff (KT), a ~4 m thick vitric ash with an anorthoclase feldspar age of 3.570 ± 0.014 Ma. This unit is widely recognized at Korsi Dora, in collection areas north of the Waki-Mille confluence and outside the field area. The KT correlates with the Lokochot Tuff of the Omo-Turkana Basin in Kenya. Sedimentological features of the mudstone and sandstone in and near the excavation site are consistent with deposition in a floodplain or floodplain lake proximal to a stream channel.

Keywords Ar–Ar dating • Sedimentological features • Geological correlations • Korsi Dora • Woranso-Mille

Introduction

KSD-VP-1/1, a partial skeleton of *Australopithecus afarensis*, was excavated from the Korsi Dora collection area in the northwestern part of the Woranso-Mille paleoanthropological study area (WORMIL). WORMIL covers an area of ~60 km by ~20 km near the western margin of the Afar depression, south of the Gura'ale volcanic center and north of the road between the towns of Mille and Bati, in northern Ethiopia (Fig. 2.1). The area was first surveyed for fossils during the early 1970s, but detailed geological and paleontological research did not begin until 2004 (Haile-Selassie et al. 2007). Geological investigations to date have focused on the northern part of the WORMIL site, where Pliocene strata are exposed in the drainage basin of the Mille River (Fig. 2.1c). The Korsi Dora collection area consists of low relief exposures of fossiliferous Pliocene strata adjacent to the Kilaytoli River, an ephemeral drainage that feeds into the Mille River.

KSD-VP-1/1 was excavated from ~49 square meters of flat lying mudstone and sandstone. The fossil horizon is ~2.6 m above a lapillistone tuff with an $^{40}Ar/^{39}Ar$ age of

B.Z. Saylor (✉)
Department of Earth, Environmental and Planetary Sciences, Case Western Reserve University, Cleveland, OH 44106, USA
e-mail: bzs@case.edu

M. Alene
Department of Geology and Geophysics, Addis Ababa University, Addis Ababa, Ethiopia
e-mail: mulugeta_alene@yahoo.com

A. Deino · G. Scott
Berkeley Geochronology Center, 2455 Ridge Road, Berkeley, CA 94709, USA
e-mail: adeino@bgc.org

G. Scott
e-mail: gscott@bgc.org

L. Gibert
Departament de Geoquímica, Petrologia i Prospecció Geològica, Universitat de Barcelona, C/Martí i Franqués s/n, 08028 Barcelona, Spain
e-mail: lgibert@ub.edu

Y. Haile-Selassie
Department of Physical Anthropology, Cleveland Museum of Natural History, 1 Wade Oval Drive, Cleveland, OH 44106, USA
e-mail: yhailese@cmnh.org

S.M. Melillo
Department of Human Evolution, Max Planck Institute for Evolutionary Anthropology, Deutscher Platz 6, 04103 Leipzig, Germany
e-mail: stephanie_melillo@eva.mpg.de

© Springer Science+Business Media Dordrecht 2016

Yohannes Haile-Selassie and Denise F. Su (eds.), *The Postcranial Anatomy of Australopithecus afarensis: New Insights from KSD-VP-1/1*, Vertebrate Paleobiology and Paleoanthropology, DOI 10.1007/978-94-017-7429-1_2

3.60 ± 0.03 Ma (2σ). The dated tuff was collected from the bottom of a trench 25 m to the north of the excavation (Haile-Selassie et al. 2010a). We expand on the results of geologic mapping and tephrochemical studies that, together with paleomagnetic data and radiometric ages, clarify the stratigraphic and structural relationships at Korsi Dora and the position of the fossil horizon relative to marker tuffs (Haile-Selassie et al. 2010a; Deino et al. 2010). These marker tuffs enable correlation of the Korsi Dora section with a longer, well-dated composite section comprising exposures near the confluence of the Waki and Mille rivers, 3.3 km northwest of Korsi Dora, and also with comparably

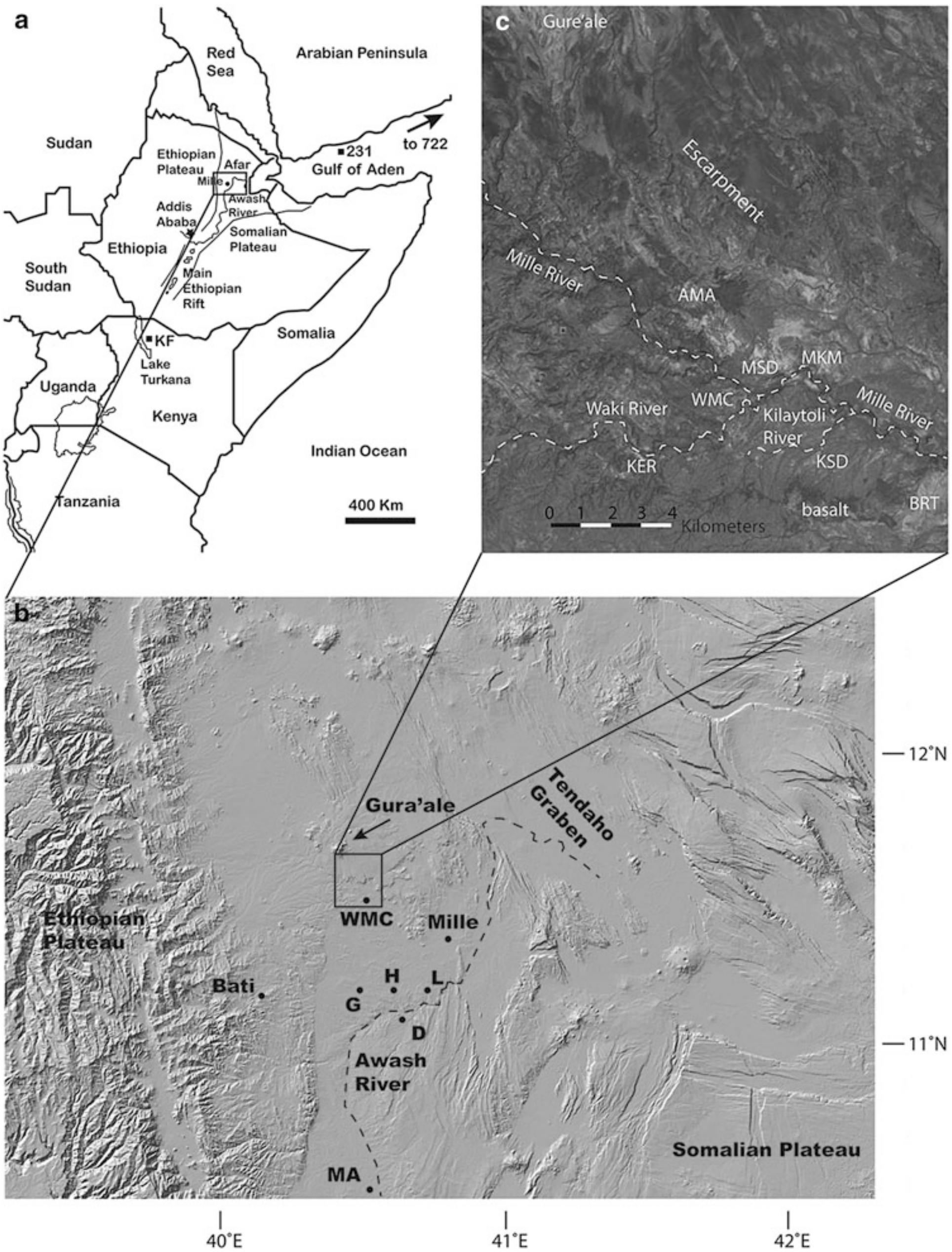

Fig. 2.1 **a** Map of the Horn of Africa and locations discussed in the text. *KF* Koobi Fora Formation; 722 and 231 are locations of deep sea cores where correlates of the Lokochot Tuff have been identified. **b** Relief map of the southwestern region of the Afar depression in Ethiopia showing the location of the Waki-Mille Confluence (WMC) in the Woranso-Mille research area relative to physiographic and tectonic features and relative to paleoanthropological research areas of the Lower and Middle Awash Valley. Base map generated from GeoMapApp (http://www.geomapapp.org) using the Global Multi-Resolution Topography Synthesis (Ryan et al. 2009). *D* Dikika; *G* Gona; *H* Hadar; *L* Ledi-Geraru; *MA* Middle Awash. **c** Map of the area around the Waki-Mille confluence (WMC) in the northern part of the Woranso-Mille study area showing the location of Korsi Dora (KSD) relative to other collection areas discussed in the text. *AMA* AmAdo; *MKM* Makah Mera; *MSD* Mesgid Dora; *KER* Kerare. Base map is a grayscale ASTER image

aged fossiliferous strata and deep-sea cores around the Horn of Africa. We also present details of the sedimentology of the excavation site and nearby exposures that provide insight into the environment of deposition and preservation of the partial skeleton.

Geologic Setting of the Woranso-Mille Study Area

WORMIL lies near the western margin of the Afar triangle (Fig. 2.1a), near the triple junction where the Main Ethiopian Rift meets the on-land propagators of the Red Sea and Gulf of Aden spreading ridges (Beyene and Abdelsalam 2005). WORMIL lies 75 km southwest of the Tendaho Graben (Fig. 2.1b), the current locus of the Red Sea propagator, where NNE-oriented normal faults associated with the Main Ethiopian Rift intersect NW-oriented faults associated with the Red Sea Rift (Acocella 2010). The Main Ethiopian Rift reached the Afar about 11 Ma. Extension along the Red Sea Rift, which began about 30 Ma, propagated into the Tendaho Graben at about 4 Ma, accompanied by a resurgence of volcanism central to rift axes, including the development of silicic volcanoes, and the emplacement of the Afar Series of basalts across much of the Afar (Acocella et al. 2008; Lahitte et al. 2003).

WORMIL shares its southern border, the Mille-Bati road, with paleoanthropological sites of the Lower Awash Valley (Fig. 2.1b). Decades of work by interdisciplinary field teams south of this border have extracted a rich fossil record from the Late Miocene to Pleistocene strata of the Awash Group (Kalb et al. 1982; Renne et al. 1999; WoldeGabriel et al. 2009). These strata, consisting of the Adu Asa (6.4 to 5.2 Ma), Sagantole (>4.6 to 3.9 Ma), Hadar (>3.8 to 2.9 Ma), and Busidima (2.7 to 0.16 Ma) Formations, filled half gra-bens that developed in response to the Main Ethiopian Rift extension and may also have been influenced by the Red Sea Rift (Quade et al. 2008; Wynn et al. 2008). Basin-bounding faults, inferred for the early stages of rift evolution, were likely discontinuous, forming structurally isolated basins. By the time of deposition of the Busidima Formation, however, faults had linked and localized along the western edge of a contiguous basin leading to axial drainage and the

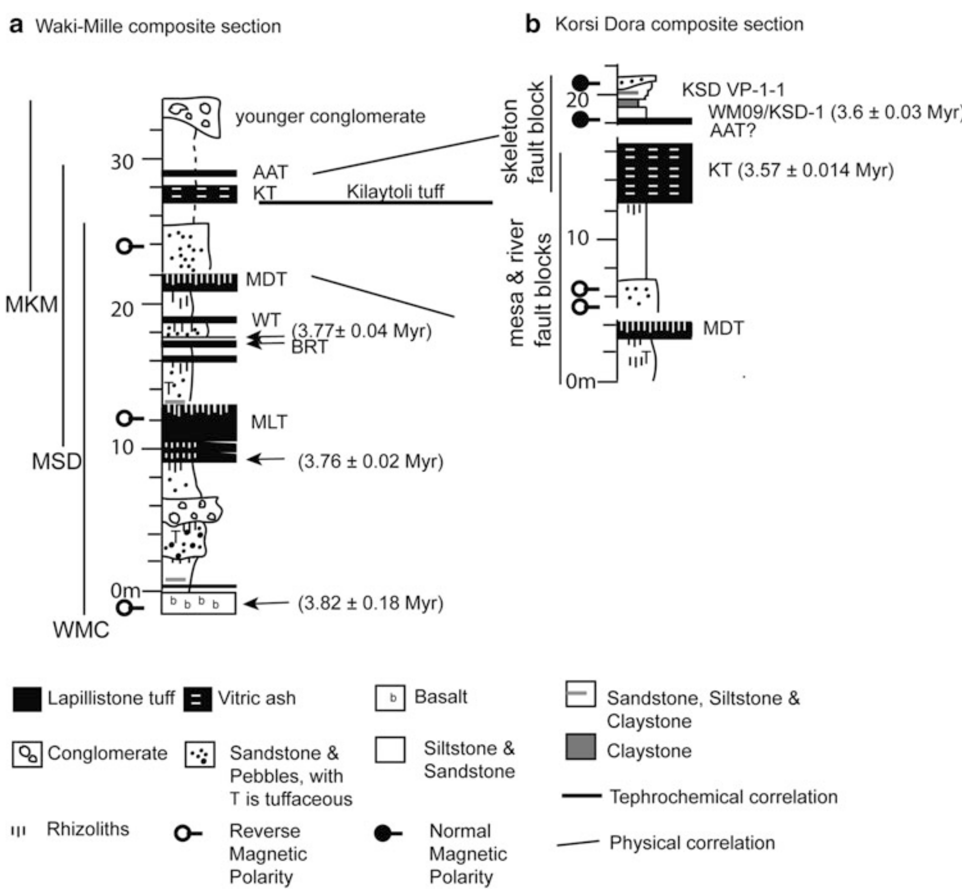

Fig. 2.2 Composite reference sections for the stratigraphy at (**a**) the Waki-Mille area, including the Waki-Mille confluence (WMC), Mesgid Dora (MSD) and Makah Mera (MKM), and (**b**) Korsi Dora (KSD). *MLT* Mille tuff sequence; *BRT* basalt-rhyolite tuff; *WT* Waki tuff; *MDT* Mesgid Dora tuff; *KT* Kilaytoli tuff; *AAT* AmAdo tuff sequence

development of the proto-Awash River (Quade et al. 2008). Thus, in addition to their rich record of Miocene–Pliocene and Pleistocene vertebrate evolution and environmental change, the formations of the Awash Group also document the volcanic and tectonic history of rifting and landscape evolution near the Afar triple junction.

The skeleton excavation site at Korsi Dora is part of a Pliocene age volcanic and sedimentary succession, exposed most extensively north of the Mille River (Deino et al. 2010). Exposures at the Waki-Mille confluence and nearby, at the Mesgid Dora and Makah Mera collection areas, constitute a well-dated composite section (Fig. 2.2), >30 m thick, of sandstone, mudstone, and conglomerate, interbedded with decimeter- to meter-scale volcanic tuffs ranging in age from ≥3.77 Ma to <3.57 Ma (Deino et al. 2010). At the confluence, the sedimentary section overlies 3.82 ± 0.18 Ma basalt (Deino et al. 2010), but more recent fieldwork has demonstrated that the tuffaceous and sedimentary strata continue below the basalt west of the confluence. Recent work has also documented the presence of additional layers of basalt within the sedimentary succession, above the confluence basalt (Alene et al. 2012). The sedimentary succession in the vicinity of the Waki-Mille confluence overlaps in age with the Basal Member of the Hadar Formation, especially as defined at Dikika (Wynn et al. 2006, 2008), but differs from the Basal Member in containing an abundance of basaltic and rhyolitic volcanic interbeds. Although tentatively considered as part of the Hadar Formation (Deino et al. 2010), it remains to be determined if strata in the Waki-Mille area, more than 40 km north of Hadar and Dikika, accumulated in a basin contiguous with that of the Basal Member.

Korsi Dora Collection Area

The Korsi Dora collection area borders the Kilaytoli River, ~2.8 km southeast of the Waki-Mille confluence. The area is named for the Korsi Dora drainage (Fig. 2.3), one of several drainages that initiate along an east–west oriented ridge of basalt, south of the Kilaytoli River, and feed northward into the Kilaytoli River or directly into the Mille River. The basaltic ridge, which extends for >10 km laterally, forms a southern boundary to exposures of tephra-rich strata typical of the Waki-Mille confluence and the surrounding area (Fig. 2.1c). The basalt is partially covered by younger conglomerate, which also covers much of Korsi Dora, obscuring the contact between basalt and topographically lower fossiliferous strata (Fig. 2.3).

For the most part, exposures of fossiliferous strata at Korsi Dora are limited to low relief outcrops, <2 m thick, where

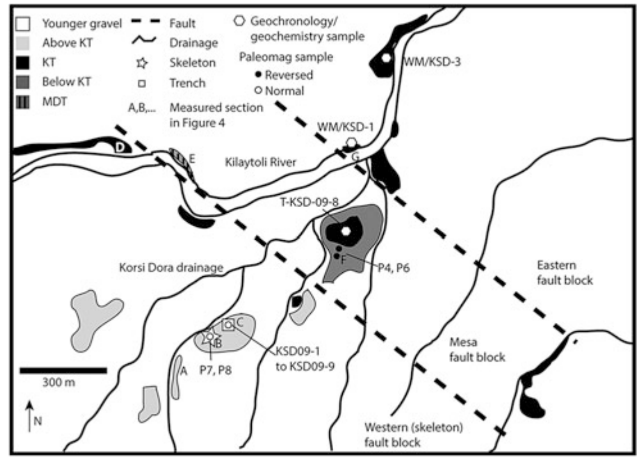

Fig. 2.3 Geologic map of the Korsi Dora area showing locations of samples and sections discussed in the text and shown in Fig. 2.4

erosion along the Korsi Dora drainage and its tributaries removed younger conglomeratic cover (Figs. 2.3 and 2.4). Thicker sections, up to 6 m, are exposed along the banks of the Kilaytoli River and on a small mesa near the river.

Stratigraphic Position of the Basalt Ridge

The approximate stratigraphic position of the basalt ridge at the southern boundary of Korsi Dora can be determined from relationships at Korsi Dora and at other nearby collection areas. Basalt in the ridge extends westward to the Kerare collection area (Fig. 2.1c) where it lies above >20 m of volcaniclastic-rich strata similar to the Waki-Mille composite section, including the Mille tuff sequence (MLT), the Basalt Rhyolite tuff (BRT), and the Waki tuff (WT) or higher (Fig. 2.2). Stratigraphically higher tuffs that are not present in the Kerare section may have been removed by erosion along a >10 m deep fluvial channel, which underlies the basalt and cuts down from a position above, at least, the WT to the level of the MLT sequence. At the eastern limits of the ridge, at Burtele, the exposure of basalt curves to the north and dips eastward under a younger (≤3.47 Ma) fossiliferous succession containing the hominin partial foot fossil BRT-VP-2/73 (Haile-Selassie et al. 2012).

These relationships constrain the basalt at Korsi Dora to a position above the WT and below the section at Burtele, but do not constrain its position relative to the Korsi Dora strata, which contain the Kilaytoli tuff (KT) and thus correlate with the part of the Waki-Mille composite section that is above the WT (Deino et al. 2010). There is, however, no evidence for strata comparable to the Korsi Dora section above the basalt ridge at Burtele or elsewhere (Haile-Selassie et al. 2012).

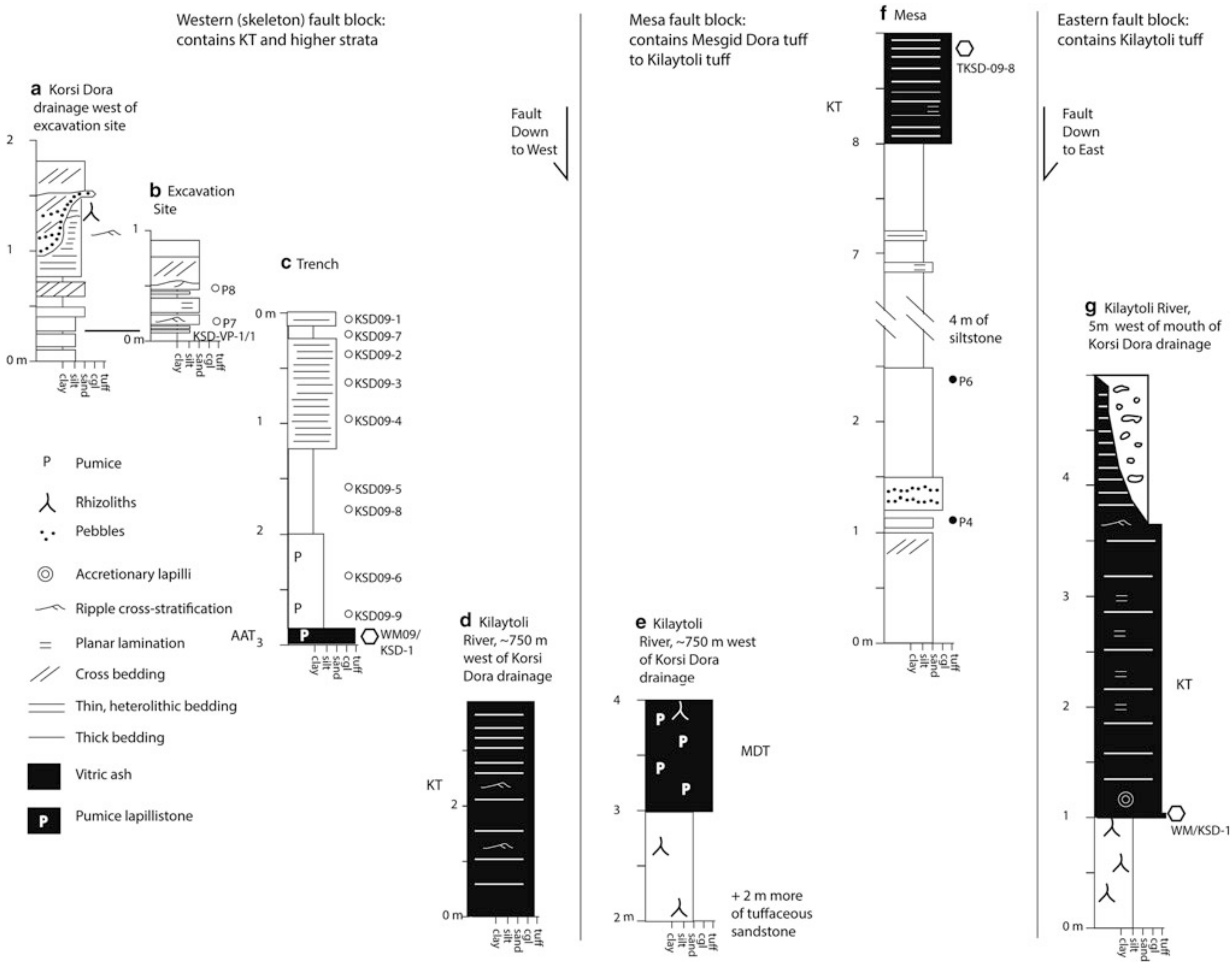

Fig. 2.4 Measured stratigraphic sections at Korsi Dora showing positions of the samples discussed in the text. For locations of sections and samples see Fig. 2.3

Also, although faults are inferred along offset linear features that define the edge of the basalt ridge, their vertical offsets appear small. The simplest interpretation is that the Korsi Dora section and the Waki-Mille composite section lie stratigraphically below the level of the Kerare-to-Burtele ridge of basalt and are older than the dated tuff at Burtele (3.460 ± 0.016 Ma, 2σ) (Haile-Selassie et al. 2012).

Kilaytoli Tuff

The Kilaytoli tuff (KT) is a white vitric ash named for exposures along the Kilaytoli River and present at several locations around Korsi Dora (Figs. 2.3 and 2.4). It is also recognized in collection areas north of the Mille River (Fig. 2.2) based on physical characteristics, stratigraphic position, $^{40}Ar/^{39}Ar$ geochronology, and glass geochemistry (Deino et al. 2010).

Where it was first described in an outcrop along the northern bank of the Kilaytoli River, 5 m west of the mouth of the Korsi Dora drainage, the KT sits on siltstone with rhizoliths (Figs. 2.4g and 2.5a). It is as much as 4 m thick but decreases to 2.6 m over the span of a few meters, truncated from above by an erosional unconformity with a younger conglomerate. A coarse crystal concentrate layer, 1 cm thick, at the base of the tuff is overlain by ∼2.6 m of thin- to thick-bedded, medium to fine vitric ash, with concentrations of accretionary lapilli, followed by ∼1.4 m of recessive weathering, thin- to medium-bedded fine ash with silt. Beds

Fig. 2.5 Outcrop photos of the Kilaytoli tuff on Korsi Dora (**a**) where it was first described in the Kilaytoli River and (**b**) on top of mesa. Photos courtesy of Elizabeth Russell

are tabular to locally trough shaped and exhibit normal grading, planar horizontal laminations, climbing ripple cross stratification, and local soft sediment deformation.

North of the Mille River, the KT has been documented at Mesgid Dora, Makah Mera, Aralee Issie, and AmAdo, where it varies from 1 to 3 m in thickness and is similar in characteristics to outcrops at Korsi Dora. It sits on siltstone that has been pedogenically modified to varying degrees. Stratigraphically, it ranges from 5 to 15 m above the MDT, a 1 to 3 m thick pumice lapillistone tuff, which is recognized in multiple collection areas and, depending on location, accumulated as either an airfall tuff or a fluvially reworked pumiceous deposit (Deino et al. 2010) (Fig. 2.2a).

At the Waki-Mille confluence and across much of Mesgid Dora, the section is truncated below the level of the KT, whereas at Aralee Issie and across much of Makah Mera, the KT is the highest preserved tuff in the section. At AmAdo, however, the section continues higher to include a pink pumice, lithic lapillistone that is 25 cm thick and 5 m above the top of the KT (Haile-Selassie et al. 2007, 2010b). Later work showed that the tuff reached as much as a meter thick in the AmAdo area and a second similar tuff was identified between it and the KT. These tuffs, which we will here refer to as the AmAdo tuff (AAT) sequence, were initially recognized only at AmAdo and were not named. More recently, however, a similar tuff has been identified 1–2 m above the KT in flats and hilltop exposures between Mesgid Dora and Makah Mera (Fig. 2.2a) and a similar pair of tuffs, which is present above the KT at the confluence of the Kilaytoli River and the Mille River. Furthermore, expansion of fieldwork has identified a physically similar pink, lithic, pumice lapillistone tuff above the KT in exposures along a laterally extensive, basalt-capped escarpment, ~2.5 km northeast of AmAdo (Fig. 2.1c). Based on their stratigraphic position and physical similarity, these tuff exposures correlate with the AAT sequence, which can now be recognized as a widespread marker horizon above the KT.

Deino et al. (2010) reported electron probe microanalysis (EPMA) data for glass shards in samples of the KT from the Kilaytoli River, Makah Mera, and Aralee Issie (Table 2.1), all of which exhibit bimodal distributions of Fe_2O_3 and Al_2O_3 concentration (Fig. 2.6). This distinctive distribution, along with a close similarity in all other measured oxides, supports the correlations made among sections based on physical characteristics and stratigraphic position.

Deino et al. (2010) reported a laser fusion $^{40}Ar/^{39}Ar$ mean age of 3.570 ± 0.014 Myr (2σ) for the KT, for anorthoclase feldspar crystals from two samples (WM-KSD-1 and WM-KSD-3) of the crystal concentrate layer at the bottom of the outcrops along the Kilaytoli River (Fig. 2.3). Based on age and glass geochemistry, the KT correlates with the Lokochot Tuff (Deino et al. 2010) and has extensive extra-basinal distribution. The Lokochot Tuff, defined in the Koobi Fora Formation east of Lake Turkana, has been correlated geochemically to tuffs at multiple sites of the Omo-Turkana Basin of Kenya and southern Ethiopia (Cerling and Brown 1982; Brown and Fuller 2008), and has also been recognized in the Gulf of Aden and the Arabian Sea (Fig. 2.1a) (Brown et al. 1992; DeMenocal and Brown 1999; Feakins et al. 2007). It is one of several tuffs from the Omo-Turkana Basin that are recognized in the Afar and in deep-sea drill cores around the Horn of Africa as the products of massive volcanic eruptions.

Here we report additional EPMA data for vitric ash (T-KSD-9-8) from the top of the mesa at Korsi Dora. Sample preparation and analysis followed Deino et al. (2010). The white, planar laminated, fine to medium grained ash, which is >1 m thick, is similar in physical characteristics to the KT (Figs. 2.4f and 2.5b) and, like the previously studied exposures, exhibits the characteristic bimodal distributions of Fe and Al oxide abundances. These patterns, along with similarities of other oxide abundances and physical characteristics, support identification of the vitric ash on top of the mesa and elsewhere at Korsi Dora as different exposures of the KT.

Table 2.1 Normalized wt% and 1σ Normalized wt% and 1 ms compositions for the KT

	N	Na_2O	MgO	Cl	CaO	K_2O	SiO_2	Al_2O_3	TiO_2	MnO	Fe_2O_3	Total	Total O*
WM-KSD-1													
Low Fe	11	2.67	0.04	0.14	0.19	5.11	77.14	11.34	0.19	0.07	3.11	99.88	92.99
1σ		0.52	0.02	0.02	0.01	0.30	1.03	0.12	0.06	0.03	0.17		
WM-KSD-3													
Low Fe	8	2.42	0.02	0.13	0.20	4.53	78.04	11.27	0.17	0.09	3.13	99.90	92.66
1σ		0.34	0.01	0.02	0.02	0.36	0.66	0.21	0.03	0.03	0.14		
High Fe	11	2.30	0.04	0.19	0.21	4.41	77.38	10.59	0.28	0.15	4.45	99.67	92.76
1σ		0.33	0.03	0.02	0.02	0.44	0.97	0.15	0.06	0.04	0.31		
ARI-08-5													
Low Fe	13	2.34	0.03	0.13	0.20	5.01	77.32	11.24	0.22	0.12	3.40	99.82	92.82
1σ		0.44	0.01	0.02	0.02	0.56	0.78	0.25	0.08	0.04	0.41		
High Fe	5	1.77	0.04	0.17	0.22	4.40	77.86	10.64	0.27	0.14	4.48	99.63	91.57
1σ		0.25	0.02	0.05	0.04	0.39	0.46	0.29	0.02	0.03	0.30		
MSD-08-13													
Low Fe	9	2.02	0.04	0.12	0.19	4.84	77.92	11.41	0.20	0.09	3.16	99.89	92.76
1σ		0.30	0.02	0.02	0.03	0.38	0.65	0.19	0.07	0.03	0.27		
High Fe	3	1.53	0.04	0.19	0.19	4.21	78.75	10.19	0.22	0.15	4.53	100.00	93.26
1σ		0.37	0.03	0.02	0.02	0.60	0.97	0.25	0.05	0.02	0.08		
AMA-09-4													
Low Fe	4	2.26	0.03	0.14	0.20	6.13	76.57	11.39	0.17	0.13	2.99	100.63	93.41
1σ		0.68	0.01	0.01	0.03	0.31	0.44	0.10	0.05	0.05	0.22		
High Fe	5	2.21	0.03	0.18	0.19	5.54	76.41	10.71	0.21	0.15	4.36	100.12	92.61
1σ		0.75	0.01	0.01	0.02	0.66	0.79	0.22	0.04	0.05	0.31		
T-KSD 09-8													
Low Fe	2	2.63	0.03	0.14	0.20	4.52	78.14	11.04	0.18	0.06	3.07	100.08	91.13
1σ		0.86	0.01	0.02	0.02	0.45	0.38	0.05	0.01	0.04	0.00		
High Fe	2	2.12	0.05	0.20	0.22	4.11	77.98	10.30	0.19	0.19	4.64	98.98	89.23
		0.16	0.06	0.03	0.05	0.06	0.85	0.23	0.12	0.03	0.13		

F abundances are below detection limits. Different matrix corrections for F yielded small differences from oxide totals previously reported in Deino et al. (2010). * indicates new data. AMA-09-4 and T-KSD-09-8 are new data

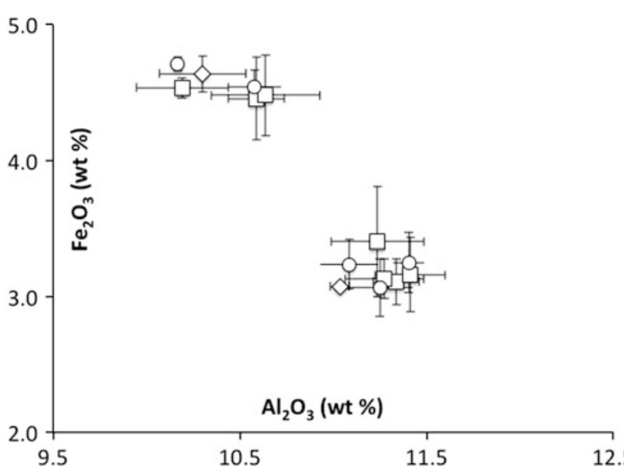

Fig. 2.6 Glass tephrochemical data (normalized, average values) for the Kilaytoli tuff and for the Lokochot Tuff of the Omo-Turkana basin showing bimodal average Fe and Al oxide abundances. Squares represent values for previously published data for samples from the Kilaytoli River and from north of the Mille River. Circles represent values for a sample of the Lokochot tuff measured at the same time as the Kilaytoli tuff. Diamonds represent new data for a sample of Kilaytoli tuff from on top of the Korsi Dora mesa

Structural Geology

The KT is an excellent chronostratigraphic marker, useful for identifying stratigraphic relationships and post-depositional structural movements of the Korsi Dora collection area (Fig. 2.3). In addition to its original description site, 5 m west of the mouth of the Korsi Dora drainage (Fig. 2.4g), the KT crops out extensively, though discontinuously, eastward, for over 1 km along the Kilaytoli River. To the west, along the Kilaytoli River, however, a span of >550 m separates the cluster of KT outcrops near the mouth of the Korsi Dora drainage from the next closest exposure of KT. There, an outcrop of KT (Fig. 2.4d) sits <5 m to the west of a short section containing a 1 m thick pumice lapillistone tuff (Fig. 2.4e). The lapillistone tuff, interpreted as MDT, has been offset along a fault to the same topographic level as the KT. South of the Kilaytoli River, the KT on top of the mesa (Fig. 2.4f) is topographically above the nearby river exposures of the tuff (Fig. 2.4g), offset by more than 6 m by a fault. Isolated bedding plane exposures of white vitric ash, similar to the KT, are also present in other drainages across the Korsi Dora area, including a drainage 700 m southeast of the mesa and a small drainage between the mesa and the excavation site (Fig. 2.3).

Topographic offset of the KT from the top of the mesa to exposures in the Kilaytoli River is the result of high angle normal faults crossing the Korsi Dora locality (Fig. 2.3). These faults contain the mesa in an uplifted horst. Exposures of KT north and east of the mesa are dropped down to the northeast, relative to the horst, along a fault that must pass between the mesa and the tuff exposures near the Korsi Dora mouth. Similarly, exposures of the KT far west of the Korsi Dora mouth, along the Kilaytoli River, are dropped down to the southwest relative to the mesa block. Placement of this second, more westerly, fault is constrained to lie between exposures of KT and MDT. Bedding plane exposures of the KT in the drainage southeast of the mesa are interpreted as part of the mesa block. By connecting the fault traces between the river exposures and the limits of these bedding plane exposures we constrain the fault trace to be approximately parallel at N 57° W. This orientation also parallels, approximately, the traces of other faults in the area.

These structural relationships place the mesa in the middle of three fault blocks. The pumice lapillistone tuff in the Kilaytoli River and the adjacent >550 m tuff-free stretch of the river are part of the mesa fault block, the relative uplift of which has exposed strata beneath the KT. The pumice lapillistone tuff, thus, is in stratigraphic position comparable to that of the MDT of the Waki-Mille composite section and, given physical similarities, is interpreted as an exposure of this tuff.

The skeleton excavation site and the trench section lie in the westernmost of the three fault blocks. This block contains exposures of the KT, specifically in the Kilaytoli River, far west of the mouth of the Korsi Dora drainage, and in a small drainage east of the trench and excavation site, but the trench section and excavation site are isolated from these exposures by younger cover (Figs. 2.3 and 2.4). Still, because the skeleton fault block is dropped down relative to the mesa block, which is capped by KT, it is expected that much of the exposures in this western block, including the excavation site, are at a stratigraphic level above that of KT.

Sedimentology and Depositional Setting

The cumulative thickness of Pliocene strata at Korsi Dora is at least 21 m. The section includes three tuffs: the KT, which is a vitric ash; a pumice lapillistone tuff, more than 8 m below the KT, which is similar in character and stratigraphic position to the MDT; and an altered lithic, pumice lapillistone tuff in the trench, which is interpreted to sit above the KT and is similar in character and stratigraphic position to the AAT. Tephrochemical correlation of the KT combined with physical and stratigraphic similarity with other tuffs support correlation of the Korsi Dora stratigraphy to the upper part of the Waki-Mille composite section, from a few meters below the level of the MDT up to a few meters above the AAT (Fig. 2.2). The stratigraphic position of the skeleton corresponds to a position above the AAT, the highest recognized tuff in the Waki-Mille composite section. Because this stratigraphic level is preserved only locally in the area, at Korsi Dora and perhaps at AmAdo and along the escarpment northeast of AmAdo, it is not yet possible to document lateral variations in facies across the region. Interpretation of the depositional environment for the skeleton must rely on local sedimentology and stratigraphy.

Sedimentary, primarily nonvolcanic, lithologies of the Korsi Dora section include sandstone, heterolithic sandstone and mudstone, siltstone, and claystone. Sandstone is present near the bottom of the Korsi Dora section, above and below the MDT (Fig. 2.4e, f), and near the top of the Korsi Dora section, above the level of the skeleton (Fig. 2.4a–c). It is medium- to thick-bedded and medium- to coarse-grained, with pebbles or tuffaceous material locally. Beds exhibit planar horizontal stratification as well as tabular and trough cross-stratification. Heterolithic sandstone and mudstone is best developed in the upper part of the Korsi Dora section, above and below the claystone layer that yielded the skeleton. It is very thin- to medium-bedded, consisting of claystone, siltstone, and fine to medium sandstone, and exhibits planar lamination and ripple cross lamination. Siltstone with minor interbeds of sandstone predominates in the mesa section between the MDT and the KT. Claystone without heterolithic interbeds is present only in the trench section.

The skeleton was excavated from a ~10 cm thick claystone layer within a section of heterolithic sandstone, siltstone, and claystone. In the trench, the heterolithic section extends about 1 m below the skeleton horizon to overlie a layer of claystone, approximately 75 cm thick. Below this claystone is about 80 cm of siltstone with dispersed pumice, underlain by altered lapillistone tuff, at the bottom of the trench. Above the skeleton horizon is about 1 m of heterolithic sandstone and mudstone that is exposed extensively in the Korsi Dora drainage and other feeder drainages west of the excavation site. Sandstone and siltstone beds have flat, non-erosive bases and, in some cases, ripple and dune forms on their tops, preserved at the base of overlying beds of claystone. Rhizoliths are rare, but locally present in sandstone beds near the top of the heterolithic section. Claystone and siltstone in the fossil horizon and elsewhere in the heterolithic assemblage contain dispersed, ~1 cm diameter, nodular, displacive evaporite minerals, likely to be gypsum. A channel surface with 75 cm of erosional relief cuts through the heterolithic sandstone and mudstone and is filled in by sandstone and pebble conglomerate, which forms an upward-fining succession composed of amalgamated trough cross-sets.

The interbedding of claystone, siltstone, and sandstone in the heterolithic section that contains the fossil horizon is indicative of episodic flow events followed by periods of quiet settling of sediment and non-accumulation. The presence of rhizoliths, although rare, indicates that between at least some of the flow events the area was colonized by plants. Whereas, the flat bed bases and the preservation of ripple and dune forms on bed tops are evidence that the episodic flows were waning, as typically happens where channelized flows spread out as they top the channel banks or otherwise enter a less restricted body. The displacive character of probable gypsum nodules in the skeletal horizon and other mudstone beds requires a diagenetic origin, rather than precipitation from the water column or at the sediment–water interface. It may be a modern diagenetic artifact, but it also could have formed early, by evaporative pumping of saline pore water through the sediment. The channelized, cross-bedded, pebbly sandstone above the heterolithic section is typical of fluvial deposition. The thick claystone below the heterolithic section, however, requires a sustained period of quiet accumulation more consistent with a lake or pond, or the distal part of a floodplain. Taken together, the sedimentological features of the mudstone and sandstone in and near the excavation site are interpreted as evidence for deposition in a floodplain or ephemeral floodplain lake, proximal to a stream channel.

The Age of KSD-VP-1/1

KSD-VP-1/1 was excavated from claystone at the bottom of a 0.9 m thick section of interbedded claystone, siltstone, and sandstone (Fig. 2.4b). The fossil horizon correlates with claystone near the top of a 3 m deep trench dug 25 m to the east of the excavation site (Fig. 2.4c). Haile-Selassie et al. (2010a) reported a laser fusion ^{40}Ar/^{39}Ar age of 3.60 ± 0.03 Myr (2σ) for anorthoclase feldspar from a >20 cm thick tuff (WM09/KSD-1) at the bottom of the trench. The tuff is an altered, lithic, pumice lapillistone, the bottom of which was not exposed by excavation. Paleomagnetic directions reported for the trench section are normal, as are directions reported for two samples (P7 and P8) from the excavation site (Fig. 2.4b), but reverse paleomagnetic directions were reported for two samples (P4 and P6) from the lower 2.5 m of the mesa section (Fig. 2.4f) (Deino et al. 2010; Haile-Selassie et al. 2010a).

The trench section (Fig. 2.4c) and the fossil excavation site (Fig. 2.4b) are interpreted as being part of the normal subchron C2An.3n, immediately above the Gauss/Gilbert paleomagnetic transition (3.596 Ma, ATNTS2004). The reverse paleomagnetic polarities in the lower part of the mesa (Fig. 2.4f) are interpreted as the continuation of a reverse magnetozone documented for the Waki-Mille composite section (Fig. 2.2), part of the reverse subchron C2Ar below the Gauss/Gilbert transition. Paleomagnetic results for a sample of the KT on top of the mesa were variable and not useful for determining direction, but Brown et al. (1978) and Hillhouse et al. (1986) reported reverse polarities for the Lokochot Tuff in the Koobi Fora Formation and its geochemical correlate, Tuff A, in the Shungura Formation. Because the KT is correlated, based on age and geochemistry, with the Lokochot Tuff (Deino et al. 2010), it is expected that the top of the mesa also falls within the reverse subchron C2Ar.

^{40}Ar/^{39}Ar geochronology is ambiguous regarding the relative placement of the KT and the tuff in the trench, as the radiometric ages are statistically indistinguishable (3.570 ± 0.014 Ma and 3.60 ± 0.03 Ma, respectively). We do not have paleomagnetic data for the trench tuff and geochemical alteration prevents glass tephrochemistry. Still, physical differences differentiate the lithic lapillistone tuff in the trench from the fine vitric ash that constitutes the KT. The simplest interpretation is that the tuff at the bottom of the trench is conformable with the rest of the trench section and that it is positioned stratigraphically above the KT. This interpretation places the trench tuff in a similar stratigraphic position to the AAT, with which it shares physical characteristics and may correlate.

The paleomagnetic evidence positioning the mesa section and the KT stratigraphically below the trench section and the fossil excavation site is consistent with the structural evidence placing the skeletal excavation location and trench in a fault block that is dropped down relative to the mesa. This placement is also consistent with stratigraphic evidence, in that beds of sandstone and pebble conglomerate in the skeleton excavation site and in laterally equivalent exposures nearby (Fig. 2.4a) are not observed above the reverse magnetozone in the mesa, or anywhere else at Korsi Dora immediately below the KT. Similarly, there is no evidence for the KT above the level of the excavation site. We conclude that a maximum age for the fossil skeleton is given by the age of the KT tuff, 3.570 ± 0.014 Ma. A minimum age is provided by the Burtele tuff (3.469 ± 0.008 Ma), which sits stratigraphically above the basalt ridge that borders Korsi Dora. Thus, the potential depositional interval for the skeleton is a time window of about 100 ka in duration.

The depositional interval can be narrowed by applying average local sediment accumulation rates to the trench section. The trench tuff, WM09/KSD-1, has a radiometric age of 3.60 ± 0.03 Ma, but the skeleton is inferred to have a position stratigraphically above the KT, with a more precise age of 3.570 ± 0.014 Ma. Using the more precise age and sediment accumulation rates of 11 cm/ka in the Waki-Mille confluence area and 30 cm/ka in the Hadar Formation (Campisano and Feibel 2007) yields an estimated age for the skeleton of 3.56 to 3.54 Ma. This age estimate differs little from a previous estimate of 3.58 Ma based on the age of the trench tuff (Deino et al. 2010), but the structural and stratigraphic relationships clarify the position of the skeleton relative to marker tuffs and most significantly to the KT and its regional correlate, the Lokochot Tuff.

Conclusions

Pliocene strata at Korsi Dora contain distinctive marker tuffs, including the KT, which is present extensively in the WORMIL collection areas along the Mille River, near the mouth of the Waki River. The KT has been correlated with the Lokochot Tuff of the Turkana Basin based on radiometric ages and glass geochemistry. Topographic offset of the KT enables identification and mapping of northwest–southeast oriented normal faults that transect Korsi Dora, forming a horst. The partial skeleton, KSD-VP-1/1, is contained within a fault block to the west of the horst and is dropped down relative to it. Strata in the fossil excavation site and a nearby trench, which extends more than 2.7 m below the excavation horizon, comprise a normal magnetozone interpreted as part of the normal subchron C2An.3n. Based on structural, stratigraphic, and paleomagnetic evidence these sections are interpreted to lie stratigraphically above, though topographically below, a reversed polarity magnetozone that constitutes the mesa at Korsi Dora and most likely extends through the level of the KT. The reverse-polarity magnetozone is part of the reverse subchron C2Ar. The fossil skeleton is younger than the KT and younger than the Gauss/Gilbert paleomagnetic transition, both regionally identifiable stratigraphic levels. Applying regional average sediment accumulation rate to the trench section yields an estimate of 3.56 to 3.54 Ma for the age of the skeleton. KSD-VP-1/1 was excavated from a 10 cm thick bed of claystone within a ~0.9 m thick section of a heterolithic claystone, siltstone, and mudstone, which is interpreted to have been deposited by episodic flows in a floodplain or floodplain lake environment that is proximal to a stream channel.

Acknowledgments We thank the Authority for Research and Conservation of Cultural Heritage of the Ministry of Culture and Tourism of Ethiopia and the National Museum of Ethiopia for field permits and general support, the Mille District Administration for facilitating our work in the area, and the Afar people of Mille, Waki, and Waytaleyta areas for their participation in fieldwork. This project was funded by the National Science Foundation (Grant # BCS-1124716, BCS-1124705, and BCS-1125157). This paper greatly benefited from helpful comments by C. Campisano and an anonymous reviewer.

References

Acocella, V. (2010). Coupling volcanism and tectonics along divergent plate boundaries: Collapsed rifts from central Afar, Ethiopia. *Geological Society of America Bulletin, 122*, 1717–1728.

Acocella, V., Abebe, B., Korme, T., & Barberi, F. (2008). Structure of Tendaho Graben and Manda Hararo Rift: Implications for the evolution of the southern Red Sea propagator in Central Afar. *Tectonics, 27*, Tc 4016.

Alene, M., Saylor, B., Mertzman, S., Deino, A., & Haile-Selassie, Y. (2012). ^{40}Ar/^{39}Ar dating and geochemistry of the Woranso-Mille Pliocene basalts, central Afar, Ethiopia. *34th International Geological Congress Brisbane*, Australia.

Beyene, A., & Abdelsalam, M. G. (2005). Tectonics of the Afar depression: A review and synthesis. *Journal of African Earth Sciences, 41*, 41–59.

Brown, F., & Fuller, C. (2008). Stratigraphy and tephra of the Kibish Formation, southwestern Ethiopia. *Journal of Human Evolution, 55*, 366–403.

Brown, F. H., Sarna-Wojcicki, A. M., Meyer, C. E., & Haileab, B. (1992). Correlation of Pliocene and Pleistocene tephra layers between the Turkana Basin of East Africa and the Gulf of Aden. *Quaternary International, 13–14*, 55–67.

Brown, F. H., Shuey, R. T., & Croes, M. K. (1978). Magnetostratigraphy of the Shungura and Usno Formations, southwestern Ethiopia: New data and comprehensive reanalysis. *Geophysical Journal of the Royal Astronomical Society, 54*, 519–538.

Campisano, C., & Feibel, C. (2007). Connecting local environmental sequences to global climate patterns: Evidence from the hominin-bearing Hadar Formation, Ethiopia. *Journal of Human Evolution, 53*, 515–527.

Cerling, T. E., & Brown, F. H. (1982). Tuffaceous marker horizons in the Koobi Fora region and the Lower Omo Valley. *Nature, 299*, 216–221.

Deino, A., Scott, G., Saylor, B., Alene, M., Angelini, J., & Haile-Selassie, Y. (2010). $^{(40)}$Ar/$^{(39)}$Ar dating, paleomagnetism, and tephrochemistry of Pliocene strata of the hominid-bearing Woranso-Mille area, west-central Afar Rift, Ethiopia. *Journal of Human Evolution, 58*, 111–126.

DeMenocal, P., & Brown, F. (1999). Pliocene tephra correlations between East African hominid localities, the Gulf of Aden, and the Arabian Sea. *Hominid Evolution and Climatic Change in Europe, 1*, 23–54.

Feakins, S. J., Brown, F. H., & DeMenocal, P. B. (2007). Plio-Pleistocene microtephra in DSDP site 231, Gulf of Aden. *Journal of African Earth Sciences, 48*, 341–452.

Haile-Selassie, Y., Deino, A., Saylor, B., Umer, M., & Latimer, B. (2007). Preliminary geology and paleontology of new hominid-bearing Pliocene localities in the central Afar region of Ethiopia. *Anthropological Science, 115*, 215–222.

Haile-Selassie, Y., Latimer, B. M., Alene, M., Deino, A. L., Gibert, L., Melillo, S. M., et al. (2010a). An early *Australopithecus afarensis* postcranium from Woranso-Mille, Ethiopia. *Proceedings of the National Academy of Sciences of the United States of America, 107*, 12121–12126.

Haile-Selassie, Y., Saylor, B. Z., Deino, A., Alene, M., & Latimer, B. M. (2010b). New Hominid Fossils From Woranso-Mille (Central Afar, Ethiopia) and Taxonomy of Early Australopithecus. *American Journal of Physical Anthropology, 141*, 406–417.

Haile-Selassie, Y., Saylor, B., Deino, A., Levin, N., Alene, M., & Latimer, B. (2012). A new hominin foot from Ethiopia shows multiple Pliocene bipedal adaptations. *Nature, 483*, 565–569.

Hillhouse, J. W., Cerling, T. E., & Brown, F. H. (1986). Magnetostratigraphy of the Koobi Fora Formation, Lake Turkana, Kenya. *Journal of Geophysical Research, 91*, 11581–11595.

Kalb, J. E., Oswald, E. B., Mebrate, A., Tebedge, S., & Jolly, C. J. (1982). Stratigraphy of the Awash Group, Middle Awash Valley, Afar, Ethiopia. *Newsletters on Stratigraphy, 11*, 95–127.

Lahitte, P., Gillot, P. Y., & Courtillot, V. (2003). Silicic central volcanoes as precursors to rift propagation: The Afar case. *Earth and Planetary Science Letters, 207*, 103–116.

Quade, J., Levin, N. E., Simpson, S. W., Butler, R., McIntosh, W. C., Semaw, S., et al. (2008). The geology of Gona, Afar, Ethiopia. In J. Quade & J. Wynn (Eds.), *The geology of early humans in the horn of Africa* (pp. 1–32). Boulder: The Geological Society of America.

Renne, P. R., WoldeGabriel, G., Hart, W. K., Heiken, G., & White, T. D. (1999). Chronostratigraphy of the Miocene-Pliocene of the Sagantole Formation, Middle Awash Valley, Afar Rift, Ethiopia. *Geological Society of America Bulletin*, *111*, 869–885.

Ryan, W. B. F., Carbotte, S. M., Coplan, J. O., O'Hara, S., Melkonian, A., Arko, R., et al., (2009). Global multi-resolution topography synthesis. *Geochemistry Geophysics Geosystems, 10*(3). doi:10.1029/2008GC002332.

WoldeGabriel, G., Hart, W. K., Renne, P. R., Haile-Selassie, Y., & White, T. D. (2009). Stratigraphy of the Adu-Asa Formation. In: Y. Haile-Selassie & G. WoldeGabriel (Eds.), Ardipithecus kadabba: *Late Miocene evidence from the Middle Awash*, Ethiopia (pp. 27–61). Berkeley: University of California Press.

Wynn, J., Alemseged, Z., Bobe, R., Geraads, D., Reed, D., & Roman, D. (2006). Geological and palaeontological context of a Pliocene juvenile hominin at Dikika, Ethiopia. *Nature, 443*, 332–336.

Wynn, J. G., Roman, D. C., Alemseged, Z., Reed, D., Geraads, D., & Munro, S. (2008). Stratigraphy, depositional environments, and basin structure of the Hadar and Busidima Formations at Dikika, Ethiopia. In J. Quade & J. Wynn (Eds.), *The geology of early humans in the horn of Africa* (pp. 87–118). Boulder: The Geological Society of America.

Springer
http://www.springer.com/978-94-017-7427-7

The Postcranial Anatomy of Australopithecus afarensis
New Insights from KSD-VP-1/1
Haile-Selassie, Y.; Su, D.F. (Eds.)
2016, XI, 191 p. 106 illus., 82 illus. in color., Hardcover
ISBN: 978-94-017-7427-7